

Solving the Navier-Stokes Equation for Thermal Reflow

Sang-Kon KIM* and Hye-Keun OH

Department of Applied Physics, Hanyang University, Ansan 426-791

(Received 12 December 2007)

For below 32-nm pattern formation, the extreme ultraviolet (EUV) and high-index fluid-based immersion ArF lithography are still under development and it is questionable whether they will be ready to timely meet resolution needs of most aggressive memory designs. Extending technology, such as resist reflow technology, appears to be a bridge option calling for serious consideration. Hence, a physical and mechanical understanding of thermal reflow is required for its better implementation and application. In this paper, resist flow is described by using a two-dimensional time-dependent Navier-Stokes equation with the mass conservation equation, which is composed of the flow of the resist, the variation of the viscosity, the reflow temperature and the reflow time. Due to an approximation based on experiment results, numerical solutions of this equation are described and the simulation results of these solutions are compared to experiment results for a contact hole pattern. In the virtual world, these simulations can predict the phenomenon of thermal reflow, such as the effects of temperature and pitch size on the contact hole patterns, with the appropriate correspondence between these mechanical parameters and the thermal reflow parameters.

PACS numbers: 85.40.Hp, 78.20.Bh, 85.40.Bh

Keywords: Lithography, Lithography simulation, Finite element method, Thermal reflow process, Chemically-amplified resist

I. INTRODUCTION

The resist reflow process is the most popular method of enhancing the resolution of pattern shrinkage. Resist reflow is a simple and cost effective method without any additional processes because it bakes the resist at a temperature above its glass transition temperature after the pattern has been developed. For below 32-nm pattern formation, thermal reflow patterning with 1.35-NA immersion is easier than high-refractive-index immersion and extreme ultraviolet (EUV) because the EUV and high-index fluid-based immersion is still under development and it is questionable whether it will be ready to timely meet resolution needs of most aggressive memory designs [1,2]. Hence, a physical and mechanical understanding of thermal reflow is required for its better implementation and application. For an example of its applications, after the embedded microchannels are formed in single-layered SU-8 by using moving-mask ultraviolet lithography [3,4], these microchannels can be made small by using thermal reflow. For pattern shrinkage, the effective factors of thermal reflow are the baking temperature, the baking time, the pitch, the pattern layout and the resist materials properties, such as viscosity, surface

tension and adhesion [5,6]. In this paper, an equation of thermal reflow, which is composed of the flow of the resist, the variation of the viscosity, the pattern density and the reflow temperature and the reflow time, is described, solved and analyzed. In terms of a comparison with the experimental results; the accuracy of its modeling and simulation is also described.

II. EXPERIMENT

An antireflective layer of an 80-nm-thick resist is coated over a silicon wafer prior to the resist process. The coated thickness is 0.37 μm . An ethylvinylether-based polymer is coated and prebaked at 100 °C for 60 s. The exposure system is an ASML-700 system with a numerical aperture (NA) of 0.6, a partial coherency (σ) of 0.4 and an attenuated phase-shift mask. Exposed wafers are baked at 110 °C for 60 s on a hot plate and developed in a 2.38-wt% tetramethyl ammonium hydroxide (TMAH) aqueous solution for 60 s. The time of resist reflow is 90 s.

Figure 1 shows experimental results of Hynix Semiconductor Inc. for various temperature and duty ratios [7,8].

*E-mail: sangkona@hotmail.com; <http://www.sangkon.info>

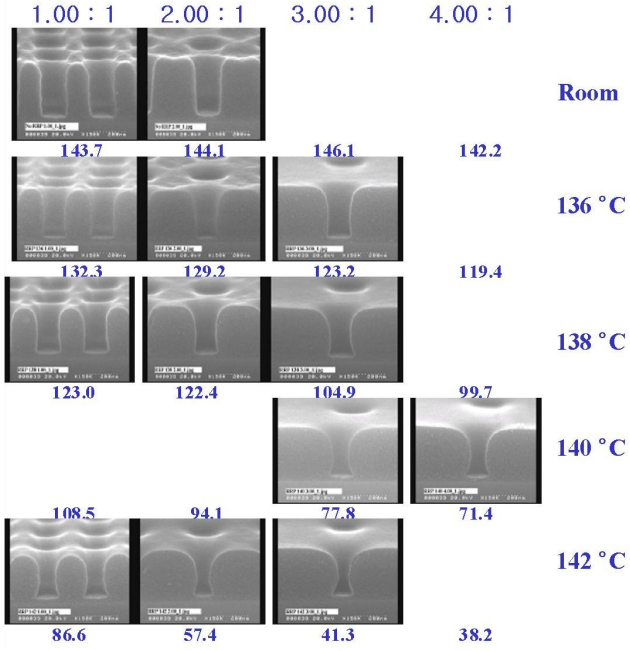


Fig. 1. Experimental results of Hynix Semiconductor Inc. for various temperatures and duty ratios [7,8].

III. MODELING OF THERMAL REFLOW

The resist reflow at temperature above its glass transition temperature can be assumed to be an ideal fluid, which is an incompressible fluid and to have a constant density (ρ) and force ($\rho \hat{n} \delta S$) exerted across a geometrical surface element $\hat{n} \delta S$ within the fluid [9]. Hence,

$$\frac{D\vec{u}}{Dt} = -\frac{1}{\rho} + g, \quad \nabla \cdot \vec{u} = 0, \quad (1)$$

where $\vec{u}(u, \phi, w)$ is the fluid velocity, g is the gravitational acceleration, ρ is the density and P is the pressure. At this point, the element of the stress tensor (T_{ij}) in an incompressible fluid is

$$T_{ij} = -\rho \delta_{ij} + \mu \left(\frac{\partial u_j}{\partial x_i} + \frac{\partial u_i}{\partial x_j} \right), \quad \nabla \cdot \vec{u} = 0. \quad (2)$$

By Eqs. (1) and (2),

$$\rho \frac{Du_i}{Dt} = -\frac{\partial P}{\partial x_i} + \mu \frac{\partial}{\partial x_j} \left(\frac{\partial u_j}{\partial x_i} + \frac{\partial u_i}{\partial x_j} \right) + \rho g_i, \quad (3)$$

$$\begin{aligned} \frac{Df}{Dt} &= \frac{\partial f}{\partial t} + \mu \frac{\partial f}{\partial x} + v \frac{\partial f}{\partial y} + w \frac{\partial f}{\partial z} \\ &\rightarrow \frac{Df}{Dt} = \frac{\partial f}{\partial t} + (\vec{u} \cdot \nabla) f. \end{aligned} \quad (4)$$

Hence, the Navier-Stokes equation is

$$\frac{\partial \vec{u}}{\partial t} + (\vec{u} \cdot \nabla) \vec{u} = -\frac{1}{\rho} \nabla P + v \nabla^2 \vec{u} + g, \quad (5)$$

$$\nabla \cdot \vec{u} = 0, \quad (6)$$

where v is the kinetic viscosity. In the x and the z directions,

$$\begin{aligned} \rho \left(\frac{\partial u}{\partial t} + u \frac{\partial u}{\partial x} + w \frac{\partial u}{\partial z} \right) \\ = -\frac{\partial P}{\partial x} + \mu \left(\frac{\partial^2}{\partial x^2} + \frac{\partial^2}{\partial z^2} \right) u + \rho g_x, \end{aligned} \quad (7)$$

$$\begin{aligned} \rho \left(\frac{\partial w}{\partial t} + u \frac{\partial w}{\partial x} + w \frac{\partial w}{\partial z} \right) \\ = -\frac{\partial P}{\partial z} + \mu \left(\frac{\partial^2}{\partial x^2} + \frac{\partial^2}{\partial z^2} \right) w + \rho g_z, \end{aligned} \quad (8)$$

$$\frac{\partial u}{\partial x} + \frac{\partial w}{\partial z} = 0. \quad (9)$$

When $\vec{u} \cdot \nabla \vec{u} \ll \mu \nabla^2 \vec{u}$ for the slow flow equation and when the gravitational acceleration (g_x) and pressure are neglected, the Navier-Stokes equation becomes the diffusion equations

$$\frac{\partial H}{\partial t} = v \frac{\partial^2 H}{\partial x^2}, \quad \text{if } u \approx H(x, t), \quad (10)$$

where H is a geometric boundary. In the shallow-water approximation, the Navier-Stokes equation becomes

$$\frac{\partial u}{\partial t} + u \frac{\partial u}{\partial x} + w \frac{\partial u}{\partial z} = -\frac{1}{\rho} \frac{\partial P}{\partial x}, \quad (11)$$

$$\frac{\partial w}{\partial t} + u \frac{\partial w}{\partial x} + w \frac{\partial w}{\partial z} = -\frac{1}{\rho} \frac{\partial P}{\partial z} - g_z, \quad (12)$$

$$\frac{\partial u}{\partial x} + \frac{\partial w}{\partial z} = 0. \quad (13)$$

From Eq. (13),

$$w = -\frac{\partial u}{\partial x} z + f(x, t) \quad (14)$$

and $f(x, t) = 0$ when $w = 0$ at $z = 0$. If $F(x, z, t) = z - H(x, t)$ in the kinematic condition at the free surface,

$$\frac{\partial F}{\partial t} + (\vec{u} \cdot \nabla) F = 0, \quad \text{at } z = H(x, t) \quad (15)$$

From Eqs. (15) and (14),

$$\frac{\partial H}{\partial t} + u \frac{\partial H}{\partial x} + H \frac{\partial u}{\partial x} = 0. \quad (16)$$

By using $c(x, t) = (gH)^{\frac{1}{2}}$ and Eq. (11),

$$\left[\frac{\partial}{\partial t} + (u - c) \frac{\partial}{\partial x} \right] (u - 2c) = 0. \quad (17)$$

When $u + 2c = 2c_0$, $z = -3c + 2c_0$ and $z \approx c \approx H(x, t)$,

$$\frac{\partial H}{\partial t} + H \frac{\partial H}{\partial x} = 0. \quad (18)$$

For an analytical solution, the gravitational acceleration (g_x) in the x-direction is zero and $\vec{u} \cdot \nabla \vec{u} \ll \mu \nabla^2 \vec{u}$ for the slow flow equations. From Eq. (7),

$$0 = -\frac{1}{\rho} \frac{\partial P}{\partial x} + v \frac{\partial^2 u}{\partial z^2} \quad \text{for } x - \text{coordinate}, \quad (19)$$

where kinetic viscosity is $v = \mu/\rho$. From Eq. (8),

$$0 = -\frac{1}{\rho} \frac{\partial P}{\partial x} - g \quad \text{for } z - \text{coordinate}. \quad (20)$$

The net upward force per unit area of surface is, by Eq. (19),

$$P - P_0 = -\mathfrak{S} \frac{\partial^2 H}{\partial x^2} \rightarrow P = -\rho g H - \mathfrak{S} \frac{\partial^2 H}{\partial x^2}, \quad (21)$$

where P is the pressure in the fluid just below the surface, P_0 is the atmospheric pressure and \mathfrak{S} is the surface tension force. If the geometric boundary function (H) is a power series, $H = 1 + x + x^2 + \dots$ and if x is smaller than 1, $H \approx 1 + x$ and

$$P = -\rho g (1 + x) - \mathfrak{S} \frac{\partial^2 H}{\partial x^2}. \quad (22)$$

From Eqs. (19) and (22),

$$u = -\left[\frac{g}{v} \frac{\partial H}{\partial x} + \frac{\mathfrak{S}}{v\rho} \frac{\partial^3 H}{\partial x^3} \right] \frac{1}{2} z^2. \quad (23)$$

From Eq. (13),

$$w_{z=H} = \frac{\partial}{\partial x} \left[\frac{g}{v} \frac{\partial H}{\partial x} + \frac{\mathfrak{S}}{v\rho} \frac{\partial^3 H}{\partial x^3} \right] \frac{1}{6} H^3. \quad (24)$$

The boundary condition is $F(x, z, t) = z - H(x, t) = 0$, so that

$$\frac{\partial H}{\partial t} = \frac{\partial}{\partial x} \left[\frac{H^3}{6} \left(\frac{g}{v} + \frac{\mathfrak{S}}{v\rho} \frac{\partial^3 H}{\partial x^3} \right) \right], \quad (25)$$

$$\frac{\partial H}{\partial \tau} = \frac{1}{6} \frac{\partial}{\partial X} \left[\Omega^{-2} \left(\frac{\partial^3 H}{\partial X^3} \right) H^3 + H^3 \right],$$

$$X \equiv \frac{x}{w}, \tau \equiv \frac{gt}{wv}, \Omega^2 \equiv \frac{\rho g w^3}{\mathfrak{S}}, \quad (26)$$

where H is the film geometry, w is the feature width, v is the kinematic viscosity of the fluid and \mathfrak{S} is the surface tension. A quasi-steady state of resist reflow can be obtained by dropping $\partial H/\partial \tau$ from Eq. (26):

$$\left(\frac{\partial^3 H}{\partial X^3} \right) H^3 + \Omega^2 H^3 = \Omega^2. \quad (27)$$

Analytical solutions with the dimensionless parameter (Ω^2) can be obtained. In the isolated contact hole, the entire domain can be divided into subdomain I of the left ridge, subdomain II of the inside ridge and subdomain III of the right ridge. The film geometries are

$$\begin{aligned} H_I &= 1 + b_1 \phi_2 + c_1 \phi_3, \\ H_{II} &= 1 \pm \frac{d}{1 + \Omega^2} + a_2 \phi_1 + b_2 \phi_2 + c_2 \phi_3 + \phi_4, \\ H_{III} &= 1 + a_3 \phi_1, \end{aligned} \quad (28)$$

where a , b and c are coefficients, which are calculated by using the boundary conditions, d is the height of resist and ϕ are the linearly independent homogenous solutions. The three linear independent homogenous solutions are

$$\begin{aligned} \phi_1 &= \exp(-\lambda x), \\ \phi_2 &= \exp(\lambda x/2) \cos\left(\lambda x \sqrt{3}/2\right), \\ \phi_3 &= \exp(\lambda x/2) \sin\left(\lambda x \sqrt{3}/2\right), \end{aligned} \quad (29)$$

$$\phi_4 = \frac{1}{3} \left[\left(1 \pm \frac{d}{1 + \Omega^2}\right) - \left(1 \pm \frac{d}{1 + \Omega^2}\right)^4 \right],$$

where in subdomains I and III , $\lambda = (3\Omega^2)^{1/3}$ and in subdomain II , $\lambda = \left[3\Omega^2 (1 \pm d(1 + \Omega^2))^{-4}\right]^{1/3}$. For the boundary condition $x = -1/2$,

$$H_I \pm d = H_{II}, \quad \frac{\partial H_I}{\partial X} = \frac{\partial H_{II}}{\partial X}, \quad \frac{\partial^2 H_I}{\partial X^2} = \frac{\partial^2 H_{II}}{\partial X^2}. \quad (30)$$

For the boundary condition $x = 1/2$,

$$H_{III} \pm d = H_{II}, \quad \frac{\partial H_{III}}{\partial X} = \frac{\partial H_{II}}{\partial X}, \quad \frac{\partial^2 H_{III}}{\partial X^2} = \frac{\partial^2 H_{II}}{\partial X^2}. \quad (31)$$

If the wafer has a topology, the thickness of the resist after thermal reflow is different due to the reflow conditions. The surface tension of the resist varies due to the nonuniformity of resist thickness. In the dense contact holes, the film geometries are

$$H_I = 1 + \frac{d}{1 + \Omega^2} + a_2 \phi_1 + b_2 \phi_2 + c_2 \phi_3 + \phi_4, \quad (32)$$

$$H_{II} = 1 + a_2 \phi_1 + b_2 \phi_2 + c_2 \phi_3. \quad (33)$$

The boundary conditions at $x = 1/2$ are

$$H_I = H_{II} + d, \quad \frac{\partial H_I}{\partial X} = \frac{\partial H_{II}}{\partial X}, \quad \frac{\partial^2 H_I}{\partial X^2} = \frac{\partial^2 H_{II}}{\partial X^2}. \quad (34)$$

The boundary conditions between $x = -1/2$ and $x = a + 1/2$ are

$$\begin{aligned} H_{II}(X=a+1/2) + d &= H_I(X=-1/2), \\ \frac{\partial H_I}{\partial X}(X=-1/2) &= \frac{\partial H_{II}}{\partial X}(X=a+1/2), \\ \frac{\partial^2 H_I}{\partial X^2}(X=-1/2) &= \frac{\partial^2 H_{II}}{\partial X^2}(X=a+1/2). \end{aligned} \quad (35)$$

IV. COMPARISON TO EXPERIMENTAL RESULTS

Figure 2 shows the numerical result of the diffusion equation in Eq. (10). The isolated pattern is wide and

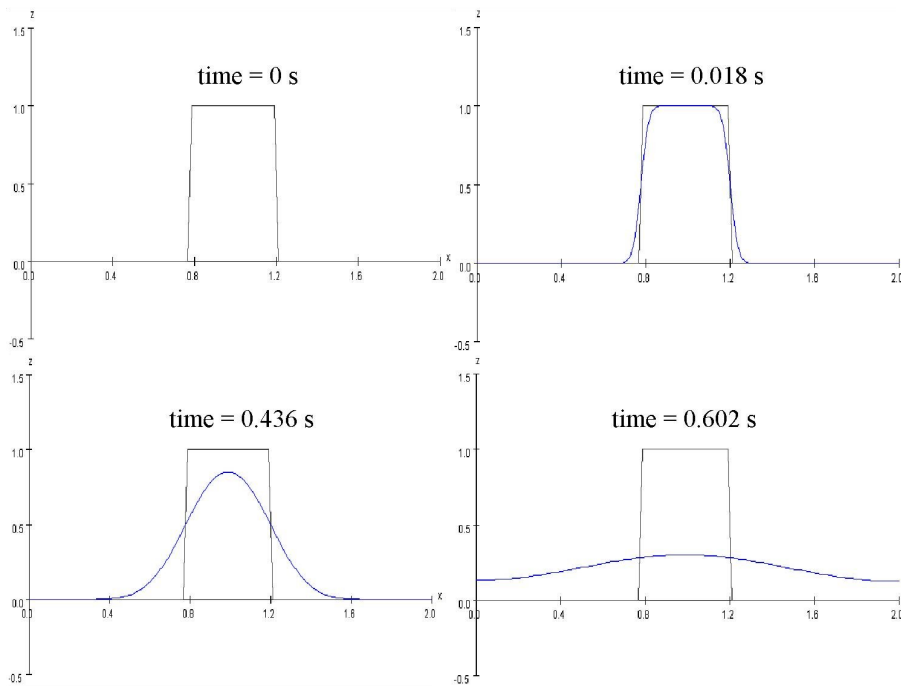


Fig. 2. Simulation results of the diffusion equation in Eq. (10) by using the second predictor-corrector scheme and the quick scheme. The isolated pattern is wider and symmetrical due to the time of thermal reflow.

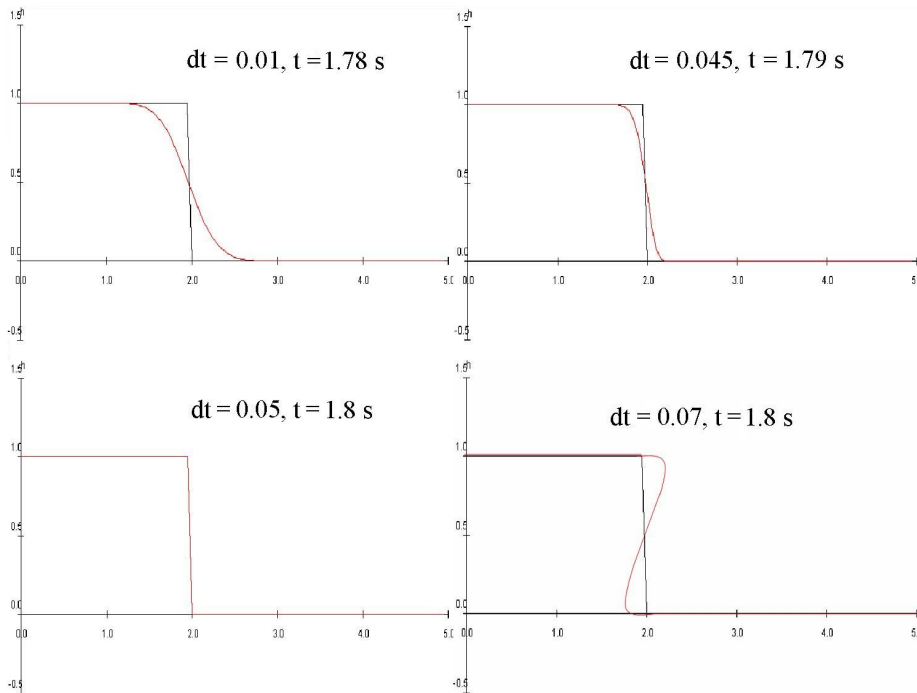


Fig. 3. Simulation flow of Eq. (18) due to Δt of the courant number, which is the reflow time interval.

symmetrical due to the time of thermal reflow. The numerical calculation methods are the second predictor-corrector scheme, the quick scheme, the forward time and centered space (FTCS) scheme and the Kawamura-Kuwahara scheme.

Figure 3 shows pattern reflow due to Δt of the courant number, which is the reflow time interval in Eq. (18). As this time interval is larger, the pattern side forms a slope of $h = -x$, a vertical slope and a slope of $h = x$. These results are the same as the experiment results.

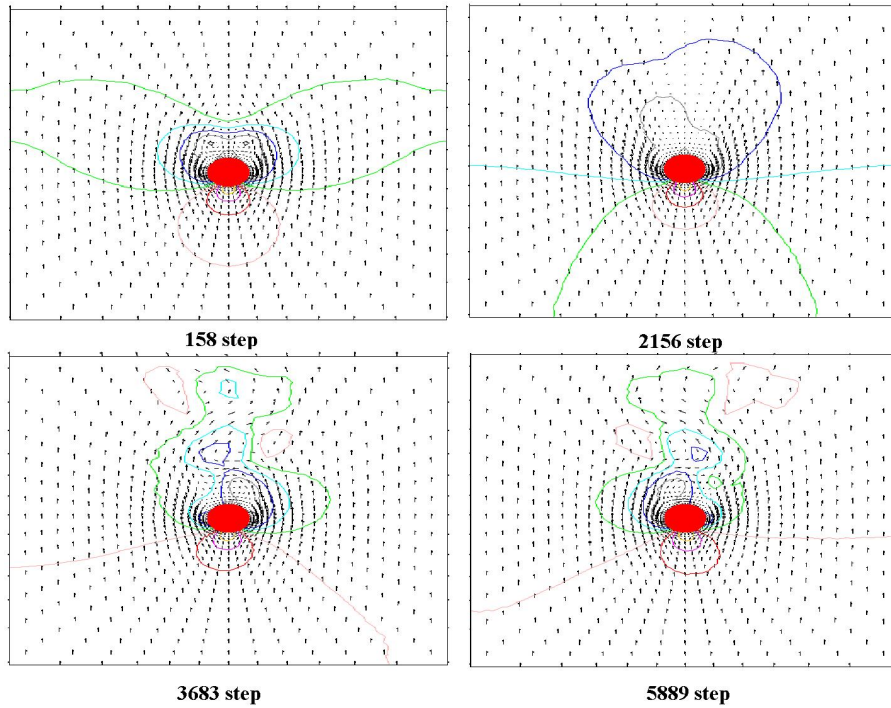


Fig. 4. Reflow velocity and pressure distributions in Eqs. (7)-(9) by using a finite element method. These results are obtained by modifying the simulation of Prof. Tomomi Uchiyama at Nagoya University, Japan.

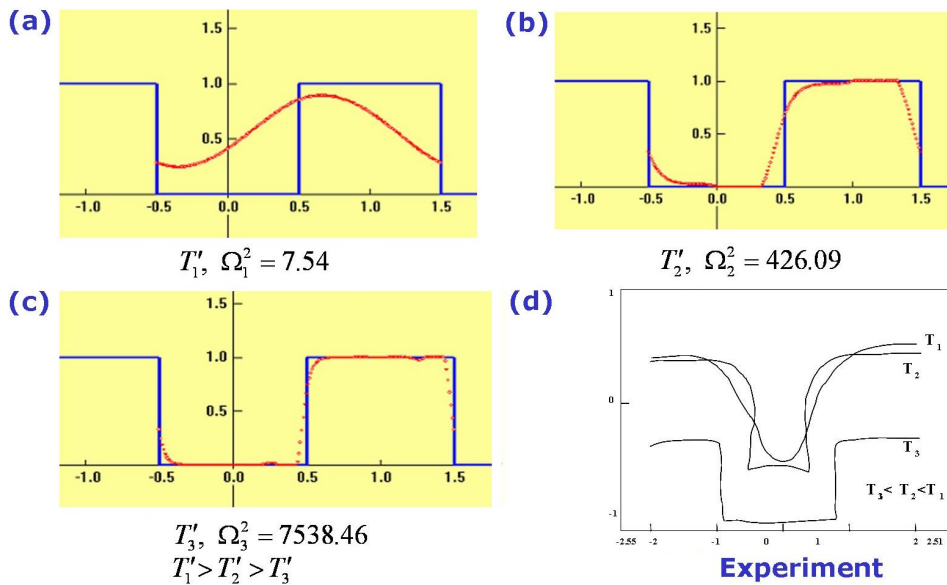


Fig. 5. Simulation results of (a) wet thermal reflow Ω_1 , (b) wet thermal reflow Ω_2 , (c) wet thermal reflow Ω_3 and (d) SEM digitization [10].

It can be assumed that the temperature of the thermal reflow causes the molecules of the to move; this high temperature corresponds to the long time interval, which is rapid reflow. The numerical calculation methods are the upstream scheme and the Lax-Wendroff scheme.

Figure 4 shows the reflow velocity and the pressure distributions of Eqs. (7)-(9) without the gravitational

acceleration, which were obtained by using a finite element method. These results are obtained by modifying the simulation of Prof. Tomomi Uchiyama at Nagoya University, Japan. The boundary conditions are $v_i = \vec{v}_i$ on the bottom, the left and the right sides and $(-p/\rho\delta_{ij} + v\partial v_i/\partial x_j)n_j = t_j$ on the top side where t is the surface tension. In Figure 4, the step corresponds

to the time of the thermal reflow, reflow velocity is described as an arrow and the pressure is described as a contour in two dimensions. Due to the steps, various velocity directions and pressure contours are shown in Figure 4.

Figures 5 (a)-(c) show wet profiles of thermal reflow according to the parameter Ω in Eq. (27). The simulation parameters are as follow: resist thickness (μm) = 0.1 and trench width (μm) = 0.1. The larger the dimensionless parameter ($\Omega_1^2 = 7.54 < \Omega_2^2 = 426.09 < \Omega_3^2 = 7538.46$, which are the surface tensions $\mathfrak{S}_3 < \mathfrak{S}_2 < \mathfrak{S}_1$ due to Eq. (26)) is, the sharper the slope of the trench area is. Figure 5 (d) shows the SEM digitization lines due to the temperature of the resist reflow process [10]. The higher the temperature is, $T_3 < T_2$, the shaper the corner edges of the resist profile are. These corners become round and collapse at temperatures above $T_1 (> T_2)$. The surface tension is the magnitude of the force that is a force of attraction between the molecules in the liquids and controls the shape of the liquid. When the temperature is increased, the surface tension is reduced because the attractive force between the molecules in the liquids is decreased and the density is reduced. As the change of density is larger than that of surface tension due to temperature, the simulation results of the dimensionless parameters ($\Omega_1 < \Omega_2 < \Omega_3$) in Figures 5(a)-(c) can describe the simulation results of temperatures ($T_1' > T_2' > T_3'$). The simulation results of temperatures can be described by the geometry of the boundary movements of the experimental results in temperatures ($T_1 > T_2$). In comparison with experiment in Figure 5(d), the simulation result is for a quasi-steady state and a wet resist state of resist reflow, so that this result excludes the time dependency and the evaporation of resist materials.

V. CONCLUSION

For an understanding of the physical and mechanical phenomenon of thermal reflow, a resist flow model is described by solving the two-dimensional time-dependent Navier-Stokes equation with the mass conservation equation. For simple approximations, numerical solutions are a diffusion solution, a non-linear wave solution in shallow-water waves, a dimensionless solution and a finite element solution with a boundary. Simulation results agree well with experimental results. In shallow-water waves, the simulation results of a non-linear wave solution are the same as a description of the vertical side views in the experimental results. In both the simula-

tion of a dimensionless solution and the experimental results, the higher the temperature is, $T_2 < T_1$, the corner edges of resist profile become rounder and more collapsed. Although the simulation parameters are not used to analyze the chemical phenomena, these simulations can predict the phenomena of thermal reflow, such as the effect of temperature and pitch size on the contact hole patterns, with an appropriate correspondence between these mechanical parameters and the thermal reflow parameters.

ACKNOWLEDGMENTS

Authors thank Kiyoshi Minemura in Aichi University of Technology and Tomomi Uchiyama in Nagoya University, Japan for their helpful researches. This research was supported by the MIC(Ministry of Information and Communication), Korea, under the ITRC(Information Technology Research Center) support program supervised by the IITA(Institute of Information Technology Advancement) (IITA-2008-C109008010030).

REFERENCES

- [1] S.-K. Kim and H.-K. Oh, J. Korean Phys. Soc. **51**, 1413 (2007).
- [2] S.-K. Kim, J. Korean Phys. Soc. **50**, 1952 (2007).
- [3] Y. Inamoto, Y. Hirai, K. Sugano, T. Tsuchiya and O. Tabata, *in the 7th International Workshop on High Aspect Ratio Micro Structure Technology (HARMST2007)* (Besancon, 2007), p. 31.
- [4] Y. Hirai, Y. Inamoto, K. Sugano, T. Tsuchiya and O. Tabata, *in the 16th International Conference on Solid-State Sensors, Actuators and Microsystems (Transducers'07)* (Lyon, 2007), p. 545.
- [5] S.-K. Kim, H.-K. Oh, I. An, S.-M. Lee, C.-K. Bok and S.-C. Moon, J. Korean Phys. Soc. **46**, 1439 (2005).
- [6] S.-K. Kim and H.-K. Oh, J. Korean Phys. Soc. **47**, S456 (2005).
- [7] C.-W. Koh, D.-H. Lee, M.-S. Kim, S.-N. Park and W.-K. Kwon, *Proc. SPIE* **5039**, 1382 (2003).
- [8] J.-S. Kim, J.-C. Jung, K.-K. Kong, G. Lee, S.-K. Lee, Y.-S. Hwang and K.-S. Shin, *Proc. SPIE* **4690**, 577 (2002).
- [9] S.-K. Kim and T. S. Kim, J. Korean Phys. Soc. **48**, 1661 (2006).
- [10] G. Thallikar, H. Liao, T. S. Cale and F. R. Myers, J. Vac. Sci. Technol. B **13** 187 (1995).